

Document downloaded from:

<http://hdl.handle.net/10251/37718>

This paper must be cited as:

López ., O.; Piñol ., P.; Martínez Rach, MO.; Pérez Malumbres, MJ.; Oliver Gil, JS. (2011). Low-Complexity 3D-DWT video encoder applicable to IPTV. *Signal Processing: Image Communication*. 26(7):358-369. doi:10.1016/j.image.2011.01.008.



The final publication is available at

<http://dx.doi.org/10.1016/j.image.2011.01.008>

Copyright Elsevier

Low-Complexity 3D-DWT video encoder suitable for IPTV

O. López^{a,*}, P. Piñol^a, M.O. Martínez-Rach^a, M.P. Malumbres^a, J. Oliver^b

^a*Miguel Hernandez University, Avda. Universidad s/n, 03202 Elche (Alicante), Spain*

^b*Universidad Politécnica de Valencia, Camino de Vera s/n, 46222 Valencia, Spain*

Abstract

3D-DWT encoders are good candidates for applications like professional video editing, IPTV video surveillance applications, live event IPTV broadcast, multi-spectral satellite imaging, HQ video delivery, etc, in order to reconstruct a frame as fast as possible. However, the main drawback of the algorithms that compute the 3D-DWT is the huge memory requirement in practical implementations. In this paper, we present a fast frame-based 3D-DWT video encoder with low memory usage. Furthermore, we evaluate the behavior of the encoding system when different separable 1D filters are applied, both in the spatial and temporal dimension.

Keywords: 3D-DWT, wavelet-based video coding, IPTV video surveillance

1. Introduction

Internet Protocol Television (IPTV) is the use of an IP broadband network to deliver television services to the end user. Nowadays, IPTV makes use of H.264 encoding [1] to deliver the media content, although MPEG-4 Part II [2] and MPEG-2 [3] encoding systems still are used. However, these encoders have a great computational complexity, specially for real-time applications or devices with power or memory consumption constraints.

In recent years, three-dimensional wavelet transform (3D-DWT) has focused the attention of the research community, most of all in areas such as

*Corresponding author

Email addresses: otoniel@umh.es (O. López), pablop@umh.es (P. Piñol), mmrach@umh.es (M.O. Martínez-Rach), mel@umh.es (M.P. Malumbres), joliver@disca.upv.es (J. Oliver)

10 video watermarking [4] and 3D coding (e.g., compression of volumetric data
11 [5] or multispectral images [6], 3D model coding [7], and specially, video cod-
12 ing). These encoders are good candidates for some applications like profes-
13 sional video editing, IPTV video surveillance applications (Traffic cameras,
14 child/day care, mall cctv surveillance), live event IPTV broadcast, multi-
15 spectral satellite imaging, HQ video delivery, etc., where a specific frame of a
16 video sequence must be reconstructed as fast as possible and with high visual
17 quality.

18 In video compression, some early proposals were based on merely apply-
19 ing the wavelet transform on the time axis after computing the 2D-DWT for
20 each frame [8]. Then, an adapted version of an image encoder can be used,
21 taking into account the new dimension. For instance, instead of the typical
22 quad-trees of image coding, a tree with eight descendants per coefficient is
23 used in [8] to extend the SPIHT image encoder [9] to 3D video coding. Other
24 strategy for video coding with time filtering is Motion Compensated Tempo-
25 ral Filtering (MCTF) [10, 11]. In these techniques, in order to compensate
26 object (or pixel) misalignment between frames, and hence avoid the signif-
27 icant amount of energy that appears in high-frequency subbands, a motion
28 compensation algorithm is introduced to align all the objects (or pixels) in
29 the frames before being temporally filtered.

30 In all these applications, the first problem that arises is the extremely high
31 memory consumption of the 3D wavelet transform if the regular algorithm
32 is used, since a group of frames must be kept in memory before applying
33 temporal filtering, and in the case of video coding, we know that the greater
34 temporal decorrelation, the greater number of frames are needed in memory.
35 Another drawback is the necessity of grouping images in small Group Of
36 Pictures (GOP) to prevent very high memory usage, because the 3D-DWT
37 must be computed along a set of images which are held in memory. This
38 video sequence division into GOPs causes boundary effects between GOPs.

39 Even though several proposals have been made to avoid the aforemen-
40 tioned problems, most of them are not general (for any wavelet transform)
41 and/or complete (the wavelet coefficients are not the same as those from
42 the usual dyadic wavelet transform). In addition, software implementation
43 is not always easy. In this paper, we propose a video encoder based on a
44 frame-by-frame 3D-DWT scheme which does not require a GOP division,
45 significantly reduces the memory usage and performs the 3D-DWT much
46 faster than traditional algorithms.

47 2. 3D-DWT with low memory usage

48 In the regular 3D-DWT, the wavelet transform is applied in the three
49 directions, i.e., in the horizontal, vertical and time directions, resulting in
50 eight first level wavelet subbands (typically named as HHL_1 , HLH_1 , HHH_1 ,
51 HLL_1 , LHL_1 , LLH_1 , LHH_1 and LLL_1). Afterwards, the same decomposi-
52 tion can be done, focusing on the lowest-frequency subband (LLL_1), achiev-
53 ing in this way a second-level wavelet decomposition, and so on (see example
54 in Figure 1(b)).

55 Because this algorithm is clearly memory-intensive, with very high mem-
56 ory requirements, and exhibits high coding delay (the whole 3D-DWT needs
57 to be computed before starting the coding stage) several alternative proposals
58 have been made.

59 Some of these alternatives are based on modifying the order in which the
60 temporal filtering is calculated. E.g., in [12] the authors propose to compute
61 the wavelet transform in the time direction with only a few frames; then the
62 resulting high-frequency frames are released as a part of the final result, and
63 the low-frequency frames are employed along with a few more frames so as to
64 continue to compute the wavelet transform in the time direction. A similar
65 example is [13], where the temporal decomposition is done by interleaving
66 frames in small groups, getting a low-frequency frame per group, which is
67 stored to be decomposed later with the low-frequency frames from the rest
68 of groups. Although both algorithms ([12] and [13]) require less memory, the
69 resulting coefficients are far from being the same as in the regular algorithm.

70 Other proposals rely on blocking algorithms [14], in which the transform
71 is computed in working subsets to reduce memory usage and exploit data
72 locality. Despite the use of overlapping techniques to avoid typical block-
73 ing artifacts, the coding efficiency decreases because the redundancy among
74 neighboring blocks is not exploited.

75 In MCTF [10][11], the temporal decomposition is usually carried out with
76 a very simple transform based on the lifting scheme [15]. When using filters
77 with only a prediction and an update step (or even sometimes the update
78 step is skipped), only a few frames need to be handled in MCTF.

79 In this section we propose an extension to a three-dimensional wavelet
80 transform of the classical line-based approach [16], which computes the 2D-
81 DWT with reduced memory consumption. In the new approach, frames are
82 continuously input with no need to divide the video sequence into GOPs.
83 Moreover, the algorithm yields slices of wavelet subbands (which we call

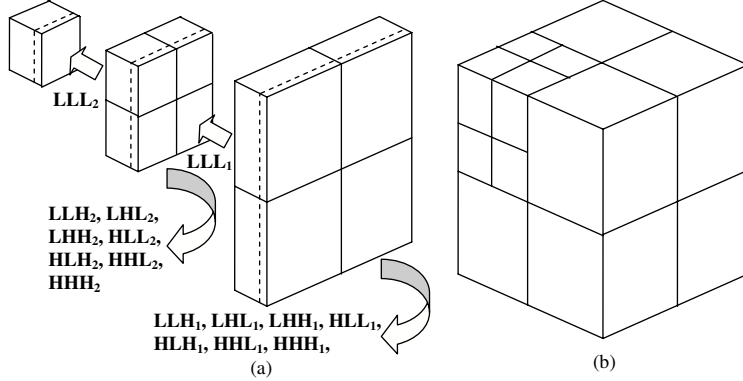


Figure 1: Overview of the 3D-DWT computation in a two-level decomposition, (a) following a frame-by-frame scheme as shown in Figure 2; or, (b) the regular 3D-DWT algorithm

84 subband frames) as soon as it has enough frames to compute them. This
 85 approach works as follows:

86 For the first decomposition level the algorithm directly receives frames
 87 one by one. On every input frame, a one-level 2D-DWT is applied. Then,
 88 this transformed image is stored in a buffer associated to the first decom-
 89 position level. This buffer must be able to keep $2N+1$ frames, where $2N+1$
 90 correspond with the number of taps for the largest analysis filter bank in the
 91 temporal direction. We only consider odd filter lengths because they have
 92 higher compression efficiency; however, this analysis could be extended to
 93 even filters as well.

94 When there are enough frames in the buffer to perform one step of a
 95 wavelet transform in the temporal direction (z -axis), the convolution process
 96 is calculated twice, first using the low-pass filter and then the high-pass filter.
 97 The result of this operation is the first frame of each high-frequency subbands
 98 (the HHL_1 , HLH_1 , HHH_1 , HLL_1 , LHL_1 , LLH_1 and LHH_1 wavelet sub-
 99 bands), and the first frame of the LLL_1 subband. At this moment, for a
 100 dyadic wavelet decomposition, we can process and release the first frame of
 101 the wavelet subbands. However, the first frame of the LLL_1 subband does
 102 not belong to the final result, since it represents the incoming data for the
 103 following decomposition level. On the other hand, once the frames at the
 104 first level buffer have been used, this buffer is shifted twice (using a rotation
 105 operation) so that two frames are discarded while another two frames are
 106 inputted at the other end. Once the buffer is updated, the process can be

107 repeated and more subband frames are obtained.

108 At the second decomposition level, its buffer is filled with the LLL_1 frames
 109 that have been computed in the first level. Once the buffer is completely
 110 filled, it is processed in the very same way as we have described for the first
 111 level. In this manner, the frames of the second level wavelet subbands are
 112 achieved, and the low-frequency frames from LLL_2 are passed to the third
 113 level. As depicted in Figure 1(a), this process can be repeated until the
 114 desired decomposition level ($nlevel$) is reached.

115 In this algorithm a major problem arises when it is implemented. This
 116 drawback is the synchronization among buffers. Before a buffer can pro-
 117 duce frames, it must be completely filled with frames from previous buffers,
 118 therefore they start working at different moments, i.e., they have different
 119 delays. Moreover, all the buffers exchange their result at different intervals,
 120 according to their level.

121 Handling several buffers with different delays and rhythms becomes a
 122 hard task. To solve the synchronization problem, the algorithm depicted
 123 at Figure 2 defines a recursive function that obtains the next low-frequency
 124 subband frame (LLL) from a contiguous level in a similar way as authors in
 [17] proposed for the 2D-DWT.

```

function LowMemUsage3D_FWT( $nlevel$ )
  set  $FramesRead_{level} = 0 \forall level \in nlevel$ 
  set  $FramesLines_{level} = \frac{Nframes}{2^{level}} \forall level \in nlevel$ 
  set  $buffer_{level} = \text{empty} \forall level \in nlevel$ 
  repeat
     $LLL = \text{GetLLLframe}(nlevel)$ 
    if ( $LLL \neq \text{EOF}$ )  $\text{ProcessLowFreqSubFrame}(LLL)$ 
  until  $LLL = \text{EOF}$ 
end of fuction

```

Figure 2: Perform the 3DFWT by calling GetLLLFrame recursive function

125
 126 The algorithm starts requesting LLL frames to the last level ($nlevel$). As
 127 seen in Figure 1, the $nlevel$ buffer must be filled with subband frames from
 128 the $nlevel-1$ level before it can generate frames. In order to get them, this
 129 function recursively calls itself until level 0 is reached. At this point, it no
 130 longer needs to call itself since it can return a frame from the video sequence,
 131 which can be directly read from the input/output system.

132 The first time that the recursive function is called at every level, it has its
 133 buffer ($buffer_{level}$) empty. Then, its upper half (from N to $2N$) is recursively
 134 filled with frames from the previous level. Recall that once a frame is received,

135 it must be transformed using a 2D-DWT before being stored. Once the upper
136 half is full, the lower half is filled by using symmetric extension. On the other
137 hand, if the buffer is not empty, it simply has to be updated. In order to
138 update it, it is shifted one position so that the frame contained in the first
139 position is discarded and a new frame can be introduced in the last position
140 ($2N$) by using a recursive call. This operation is repeated twice.

141 However, if there are no more frames in the previous level, this recursive
142 call will return End Of Frame (EOF). That points out that we are about to
143 finish the computation at this level, but we still need to continue filling the
144 buffer. We fill it by using symmetric extension again.

145 Once the buffer is filled or updated, both high-pass and low-pass filter
146 banks for the time direction (z -axis) are applied to the frames in the buffer.
147 As a result of the convolution, we get a frame of every wavelet subband at this
148 level, and an *LLL* frame. The high-frequency coefficients are compressed and
149 this function returns the LLL frame which is the lowest frequency subband
150 frame (see Figure 3).

151 The inverse DWT algorithm is similar to the forward DWT, but ap-
152 plied in reverse order. The decoding process begins immediately by filling
153 up the highest-level buffer (*nlevel*) with the information received from the
154 bit-stream. During this process, other information from the bit-stream is
155 ignored. Afterwards, once this buffer is full, we also begin to accept infor-
156 mation from the previous level, and so forth, until all the buffers are full. At
157 that moment, the video can be sequentially decoded as usual. The latency of
158 this process is deterministic and depends on the filter length and the number
159 of decomposition levels (the higher they are, the higher latency). However,
160 for the regular 3D algorithm, the latency depends on the remaining number
161 of frames in the current group when the process begins, and the GOP size. A
162 drawback that has not been considered yet is the need to reverse the order of
163 the subbands, from the forward DWT to the inverse one. This problem can
164 be solved by using some buffers at both ends, so that data are supplied in the
165 right order [16]. Other simpler solutions are to save every level in secondary
166 storage separately so that it can be read in a different order or to keep the
167 compressed bit-stream in memory if the 3D-DWT is used for compression.

168 **3. Run-Length encoder**

169 In order to have low memory consumption, once a wavelet subband is
170 calculated, it has to be encoded as soon as possible to release memory. The

```

function GetLLLFrame (level)
1) First base case: No more frames to read at this level
   if FramesReadlevel = MaxFrameslevel
       return EOF
2) Second base case: The current level belongs
to the space domain and not to the wavelet domain
   else if level = 0
       return InputFrame()
   else
3) Recursive case
3.1) Recursively fill or update the buffer for this level
   if bufferlevel is empty
       for i = N . . . 2N
           bufferlevel(i) = 2DFWT(GetLLLframe(level - 1))
       SymmetricExtension(bufferlevel)
   else
       repeat twice
           Shift(bufferlevel)
           frame = GetLLLframe(level - 1)
           if frame = EOF
               bufferlevel(2N) = SymmetricExtension(bufferlevel)
           else
               bufferlevel(2N) = 2DFWT(frame)
3.2) Calculate the WT for the time direction from the frames
in buffer, then process the resulting high frequency subband frames
   {LLL, LLH, LHL, LHH} = Z-axis_FWT_LowPass(bufferlevel)
   {HLL, HLLH, HHL, HHH} = Z-axis_FWT_HighPass(bufferlevel)
   ProcessSubFrames({LLH, LHL, LHH, HLL, HLLH, HHL, HHH})
   set FramesReadlevel = FramesReadlevel + 1
   return LLL
end of fuction

```

Figure 3: GetLLLFrame Recursive function

171 encoder cannot use global video information since it does not know the whole
172 video. Moreover, we aim at fast execution, and hence no R/D optimization
173 or bitplane processing can be applied, because it would turn it even slower.
174 In the next subsection, a Run-Length Wavelet (RLW) encoder with the afore-
175 mentioned features is proposed.

176 3.1. Fast run-length coding

177 In the proposed coding algorithm, the quantization process is performed
178 by two strategies: one coarser and another finer. The finer one consists
179 on applying a scalar uniform quantization to the coefficients using the Q
180 parameter. The coarser one is based on removing bit planes from the least
181 significant part of the coefficients. We define *rplanes* as the number of less
182 significant bits to be removed, and we call significant coefficient to those
183 coefficients $c_{i,j}$ that are different to zero after discarding the least significant

184 $rplanes$ bits, in other words, if $c_{i,j} \geq 2^{rplanes}$. The wavelet coefficients are
185 encoded as follows. The coefficients in the subband buffer are scanned row
186 by row (to exploit their locality). For each coefficient in that buffer, if it
187 is not significant, a run-length count of insignificant symbols at this level
188 is increased (run_length_L). However, if it is significant, we encode both the
189 count of insignificant symbols and the significant coefficient, and run_length_L
190 is reset.

191 The significant coefficient is encoded by means of a symbol indicating the
192 number of bits required to represent that coefficient. An arithmetic encoder
193 with two contexts is used to efficiently store that symbol. As coefficients in
194 the same subband have similar magnitude, an adaptive arithmetic encoder
195 is able to represent this information in a very efficient way. However, we still
196 need to encode its significant bits and sign. They are raw encoded to speed
197 up the execution time.

198 In order to encode the count of insignificant symbols, we encode a *RUN*
199 symbol. After encoding this symbol, the run-length count (run_length_L) is
200 stored in a similar way as in the significant coefficients. First, the number
201 of bits needed to encode the run value is arithmetically encoded (with a
202 different context), afterwards the bits are raw encoded.

203 Instead of using run-length count symbols, we could have used a single
204 symbol to encode each insignificant coefficient. However, we would need to
205 encode a larger amount of symbols, and therefore the complexity of the algo-
206 rithm would increase (most of all in the case of large number of insignificant
207 contiguous symbols, which usually occurs in moderate to high compression
208 ratios). However, the compression performance is increased if a specific sym-
209 bol is used for every insignificant coefficient, since an arithmetic encoder
210 processes more efficiently many likely symbols than a lower amount of less
211 likely symbols. So, for short run-lengths, we encode a *LOWER* symbol for
212 each insignificant coefficient instead of coding a run-length count symbol for
213 all the sequence. The threshold to enter the run-length mode and start using
214 run-length count symbols is defined by the *enter_run_mode* parameter. The
215 formal description of the depicted algorithm can be found in Figure 4.

216 4. Results

217 4.1. Wavelet Filter Evaluation

218 In this section we analyze the behavior of the proposed encoder (3D-
219 RLW) and we evaluate the performance when we use different separable 1D

```

function RLW_Code_Subband(Buffer, L)
  Scan Buffer in horizontal raster order
  for each  $C_{i,j}$  in Buffer
     $nbits_{i,j} = \lceil \log_2(|C_{i,j}|) \rceil$ 
    if  $nbits_{i,j} \leq rplanes$ 
      increase run_LengthL
    else
      if  $run\_Length_L \leq enter\_run\_mode$ 
        repeat run_LengthL times
          arithmetic_output LOWER
        else
          arithmetic_output RUN
           $rbits = \lceil \log_2(run\_Length_L) \rceil$ 
          arithmetic_output rbits
          output  $bit_{nbits_{i,j}-1}(|C_{i,j}|) \dots bit_{rplane+1}(|C_{i,j}|)$ 
          output  $sign(c_{i,j})$ 
      end of fuction
  Note: bitn(C) is a function that returns the nth bit of C

```

Figure 4: Run-length coding of the wavelet coefficients

220 filters in both spatial and temporal domain. For our simulation we have
 221 three different options for the 3D decomposition, as shown in Table 1. The
 222 first one, D97-D97, uses Daubechies 9/7F filter in both spatial and temporal
 223 dimension. The second one, D97-B53, uses Daubechies 9/7F filter for the
 224 spatial dimension and LeGall B5/3 filter for the temporal dimension. Finally,
 225 the B53-B53 option uses the LeGall B5/3 filter for both spatial and temporal
 226 dimension. We will compare the three 3D-RLW encoder versions versus the
 227 fast M-LTW Intra video encoder [18], in terms of R/D performance and
 memory requirements.

Option	Spatial	Temporal
D97-D97	Daubechies 9/7F	Daubechies 9/7F
D97-B53	Daubechies 9/7F	LeGall B5/3
B53-B53	LeGall B5/3	LeGall B5/3

Table 1: Filter choices for 3D decomposition of video

228
 229 In this new algorithm (frame-by-frame 3D wavelet transform), each buffer
 230 must be able to keep either $2N + 1$ low frequency frames at every level
 231 (recall that $2N + 1$ is the filter length), or even less if the lifting scheme is
 232 used as shown in [17]. As presented in Figure 1(a), each buffer at a level i
 233 needs a quarter of coefficients if compared with the previous decomposition
 234 level $(i - 1)$. Therefore, for a frame size of $(w \times h)$ and an $nlevel$ time

Format/Codec	QCIF	CIF	ITU-D1	Full-HD
D97-D97	3908	12548	22508	129750
D97-B53	3412	10476	16076	89292
B53-B53	3412	10476	16076	89292
M-LTW	1104	1540	4900	23800

Table 2: Memory requirements for evaluated filters (KB) (results obtained with Windows XP task manager, peak memory usage index)

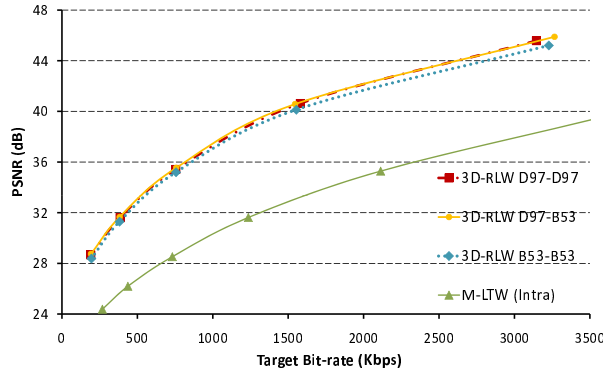


Figure 5: PSNR (dB) for all evaluated filters for Container sequence in CIF format

235 decomposition, the number of coefficients required by this algorithm is:

$$\begin{aligned}
 & (2N + 1) \times (w \times h) + (2N + 1) \times (w \times h) / 4 \\
 & + \dots + (2N + 1) \times (w \times h) / 4^{n_{level}-1}
 \end{aligned} \tag{1}$$

236 which is asymptotically (as n_{level} approaches infinity) independent of
 237 the number of frames to be encoded, less than the regular case, which needs
 238 $(w \times h \times G)$, being G the number of frames in a GOP.

$$\sum_{n=0}^{\infty} \frac{(2N + 1) \times (w \times h)}{4^n} = (2N + 1) \times (w \times h) \times \frac{4}{3} \tag{2}$$

239 For an objective evaluation, in Table 2, the memory requirements of dif-
 240 ferent encoders under test are shown. Obviously, the M-LTW encoder only
 241 uses the memory needed to store one frame. The 3D-RLW version using
 242 LeGall 5/3 temporal filter requires up to 1.5 times less memory than the one
 243 using Daubechies 9/7F time filter.

244 Regarding R/D, in Figure 5 we can see the behavior of all evaluated en-
245 coders. As shown, the 3D-RLW version using LeGall B5/3 filter in both
246 spatial and temporal domain obtains slightly lower R/D performance com-
247 pared to the other 3D-RLW versions using Daubechies 9/7F filter in the
248 spatial domain. It is interesting to see the improvement of 3D-RLW versions
249 when compared to an INTRA video encoder (up to 9 dB). In these encoders
250 no ME/MC stage is included, so the improvement is accomplished by ex-
251 ploiting only the temporal redundancy among video frames when applying
252 the 3D-DWT.

253 Among the three 3D-RLW versions, the one using Daubechies 9/7F filter
254 for the spatial domain and LeGall 5/3 filter for the temporal domain (D97-
255 B53) shows the best trade off between R/D (similar behavior than the one
256 using Daubechies 9/7F filter in the temporal domain) and memory require-
257 ments (up to 1.5 less memory than the one using Daubechies 9/7F filter in
258 the temporal domain).

259 4.2. Global Evaluation

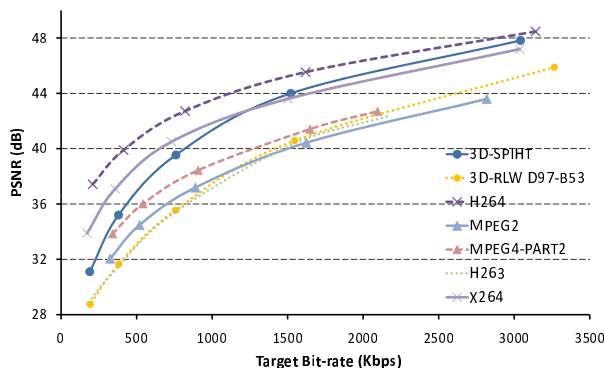
260 For an extensive evaluation, in this section we analyze the behavior of
261 the proposed encoder (3D-RLW) using Daubechies 9/7F filter for the spa-
262 tial domain and LeGall 5/3 filter for the temporal domain (D97-B53). We
263 will compare the 3D-RLW encoder versus 3D-SPIHT [19], H.264 (JM16.1
264 version), H.263 (ffmpeg-r25117), MPEG-2 (ffmpeg-r25117), MPEG-4 Part
265 II (ffmpeg-r25117) and X.264 (mingw32-libx264 r1713-1 high quality profile)
266 [20] in terms of R/D performance, coding and decoding delay and mem-
267 ory requirements. All the evaluated encoders have been tested on an Intel
268 PentiumM Dual Core 3.0 GHz with 2 Gbyte RAM memory.

269 It is important to remark that H.263, MPEG-2, MPEG-4 and X.264
270 evaluated implementations are fully optimized, using CPU capabilities like
271 Multimedia Extensions 2 (MMX2), Single Instruction Multiple Data Exten-
272 sion 2 (SSE2Fast), Supplemental Streaming SIMD Extension 3 (SSSE3) and
273 multithreading, whereas 3D-SPIHT and 3D-RLW are not optimized imple-
274 mentations.

275 In Table 3, the memory requirements of different encoders under test are
276 shown. Obviously, encoders like MPEG-2, H.263 and MPEG-4 only using P
277 frames, require to keep in memory just 2 frames to accomplish the ME/MC
278 stage, whereas encoders based on 3D-DWT like 3D-SPIHT and 3D-RLW
279 need to keep more frames in memory to apply the time filter. The 3D-RLW
280 encoder uses up to 7 times less memory than 3D-SPIHT, up to 14 times less

Format/Codec	QCIF	CIF	ITU-D1	Full-HD
H264	35824	86272	227620	489960
X264	10752	36468	36600	178940
3D-RLW	3412	10476	16076	89292
3D-SPIHT	10152	34504	118460	645720

Table 3: Memory requirements for evaluated encoders (KB) (results obtained with Windows XP task manager, peak memory usage index)



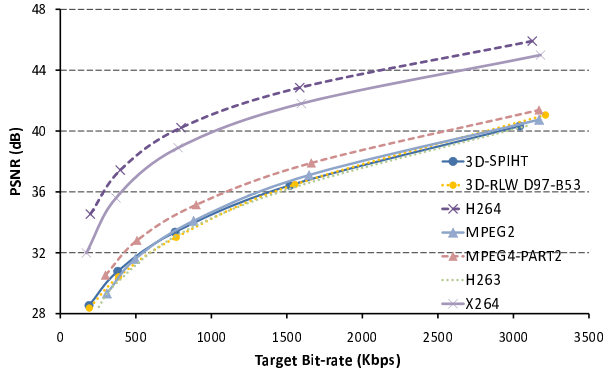
(a) Container

Figure 6: PSNR (dB) for all evaluated encoders for Container sequence in CIF format

281 memory than H.264 for ITU-D1 sequence size and up to 3 times less memory
 282 than X.264 which is an optimized version of H.264.

283 Regarding R/D, in Figures 6 and 7 we can see the R/D behavior of
 284 all evaluated encoders. As shown, H.264 is the one that obtains the best
 285 results, mainly due to the exhaustive motion estimation/motion compensa-
 286 tion (ME/MC) stage included in this encoder, contrary to 3D-SPIHT and
 287 3D-RLW that do not include any ME/MC stage. The optimized version of
 288 H.264 (X.264) has lower R/D performance than H.264 because it uses a fast
 289 ME/MC stage which is less accurate than the used in the H.264 standard
 290 version (up to 3 dB). The R/D behavior of 3D-SPIHT and 3D-RLW is sim-
 291 ilar for images with moderate-high motion activity, but for sequences with
 292 low movement, 3D-SPIHT outperforms 3D-RLW, showing the power of tree
 293 encoding system. The proposed encoder (3D-RLW) has a similar behavior
 294 than H.263 and MPEG-2 and slightly lower performance than MPEG-4.

295 Regarding coding delay, in Figure 8 we can see that the 3D-RLW encoder



(b) Foreman

Figure 7: PSNR (dB) for all evaluated encoders for Foreman sequence in CIF format

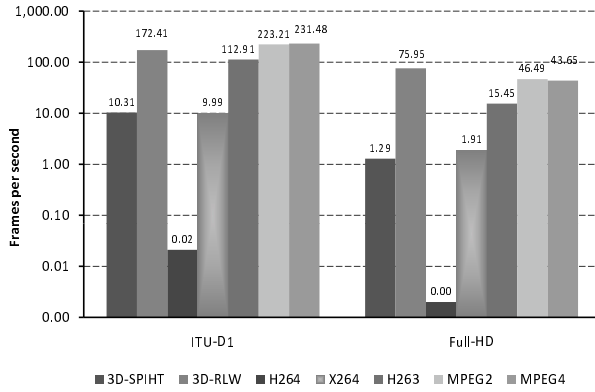


Figure 8: Execution time comparison of the encoding process

296 is one of the fastest encoders, being up to 16 times faster than 3D-SPIHT
 297 for ITU-D1 size sequences, 1.5 times faster than MPEG-2 for Full-HD size
 298 sequences and up to 39 times faster than X.264 for Full-HD size sequences.
 299 The decoding process is also very fast in 3D-RLW, having a similar behavior
 300 than MPEG-2 and MPEG-4 encoders for Full-HD size sequences.

301 5. Conclusions

302 In this paper a fast and low memory demanding 3D-DWT encoder has
 303 been presented and several separable 1D filters has been tested. The new
 304 encoder using Daubechies 9/7F for the spatial domain and LeGall 5/3 fil-
 305 ter for the temporal domain (D97-B53), reduces the memory requirements

306 compared with 3D-SPIHT (7 times less memory), H.264 (up to 14 times less
307 memory) and X.264 (up to 3 times less memory). The new 3D-DWT encoder
308 is faster than 3D-SPIHT (up to 16 times faster for Full-HD), MPEG-2 (up to
309 1.5 times faster for Full-HD) and X.264 (up to 39 times faster for Full-HD).

310 Regarding R/D, our proposal has a similar behavior than MPEG-2 and
311 H.263 and slightly lower performance than MPEG-4. When compared with
312 3D-SPIHT, our proposal has a similar behavior for sequences with medium
313 and high movement, but lower performance for sequences with low movement
314 like Container. In order to improve the coding efficiency, an ME/MC stage
315 could be added. In this manner, the objects/pixels of the input video se-
316 quence will be aligned, and so, fewer frequencies would appear at the higher
317 frequency subbands, improving the compression performance. Also, a full
318 optimization process exploiting the parallel capabilities of modern proces-
319 sors (like multithreading and SIMD instructions) will make 3D-RLW even
320 faster.

321 The low memory requirements and the fast coding/decoding process,
322 makes the 3D-LTW encoder a good candidate for IPTV applications where
323 the coding delay is critical for proper operation.

324 6. Acknowledgements

325 Thanks to Spanish Ministry of education and Science under grants DPI2007-
326 66796-C03-03 for funding.

327 References

- 328 [1] I. 14496-10, I. R. H.264, Advanced video coding (2003).
- 329 [2] ISO/IEC JTC1. ISO/IEC 14496-2, Coding of audio-visual objects (April
330 2001).
- 331 [3] ISO/IEC JTC1. ISO/IEC 13818-2, Generic coding of moving pictures
332 (2000).
- 333 [4] P. Campisi, A. Neri, Video watermarking in the 3D-DWT domain us-
334 ing perceptual masking, in: IEEE International Conference on Image
335 Processing, 2005, pp. 997–1000.

- 336 [5] P. Schelkens, A. Munteanu, J. Barbariend, M. Galca, X. Giro-Nieto,
337 J. Cornelis, Wavelet coding of volumetric medical datasets, *IEEE Trans-*
338 *actions on Medical Imaging* 22 (3) (2003) 441–458.
- 339 [6] P. Dragotti, G. Poggi, Compression of multispectral images by three-
340 dimensional SPITH algorithm, *IEEE Transactions on Geoscience and*
341 *Remote Sensing* 38 (1) (2000) 416–428.
- 342 [7] M. Aviles, F. Moran, N. Garcia, Progressive lower trees of wavelet coef-
343 ficients: Efficient spatial and SNR scalable coding of 3D models, *Lecture*
344 *Notes in Computer Science* 3767 (2005) 61–72.
- 345 [8] B. Kim, Z. Xiong, W. Pearlman, Low bit-rate scalable video coding with
346 3D set partitioning in hierarchical trees (3D SPIHT), *IEEE Transactions*
347 *on Circuits and Systems for Video Technology* 10 (2000) 1374–1387.
- 348 [9] A. Said, A. Pearlman, A new, fast and efficient image codec based on
349 set partitioning in hierarchical trees, *IEEE Transactions on Circuits,*
350 *Systems and Video Technology* 6 (3) (1996) 243–250.
- 351 [10] A. Secker, D. Taubman, Motion-compensated highly scalable video com-
352 pression using an adaptive 3D wavelet transform based on lifting, *IEEE*
353 *International Conference on Image Processing* (2001) 1029–1032.
- 354 [11] P. Cheng, J.W. Woods, Bidirectional MC-EZBC with lifting implementa-
355 tion, *IEEE Transactions on Circuits and Systems for Video Technology*
356 (2004) 1183–1194.
- 357 [12] E. Moyano, F. Quiles, A. Garrido, L. Orozco-Barbosa, J. Duato, Ef-
358 ficient 3D wavelet transform decomposition for video compression, in:
359 *Int. Work. Digital and Computational Video*, 2001.
- 360 [13] Y. Nian, L. Wu, S. He, Y. Gu, A new video coding based on 3D wavelet
361 transform, in: *IEEE International Conference on Intelligent Systems*
362 *Design and Applications*, 2006.
- 363 [14] G. Bernabe, J. Gonzalez, J. Garcia, Memory conscious 3D wavelet trans-
364 form, in: *Euromicro Conference*, 2002.
- 365 [15] W. Sweldens, The lifting scheme: a custom-design construction of
366 biorthogonal wavelets, *Applied and Computational Harmonic Analysis*
367 3 (2) (1996) 186–200.

- 368 [16] C. Chrysafis, A. Ortega, Line-based, reduced memory, wavelet image
369 compression, *IEEE Transactions on Image Processing* 9 (3) (2000) 378–
370 389.
- 371 [17] J. Oliver, E. Oliver, M.P.Malumbres, On the efficient memory usage in
372 the lifting scheme for the two-dimensional wavelet transform computa-
373 tion, in: *IEEE International Conference on Image Processing*, 2005, pp.
374 485–488.
- 375 [18] O. Lopez, M. Martinez-Rach, P. Piñol, M. Malumbres, J.Oliver, M-
376 LTW: A fast and efficient intra video codec, *Signal Processing: Image*
377 *Communication* (23) (2008) 637–648.
- 378 [19] B. Kim, Z. Xiong, W. Pearlman, Very low bit-rate embedded video
379 coding with 3D set partitioning in hierarchical trees (3D SPIHT) (1997).
- 380 [20] [http://ffmpeg.arrozcru.org/autobuilds/blog/2010/09/14/ffmpeg-](http://ffmpeg.arrozcru.org/autobuilds/blog/2010/09/14/ffmpeg-r25117-swscale-r32222-ok/)
381 [r25117-swscale-r32222-ok/](http://ffmpeg.arrozcru.org/autobuilds/blog/2010/09/14/ffmpeg-r25117-swscale-r32222-ok/), *ffmpeg* (September 2010).